

2 Literature Review

Combustion instability research dates to before the turn of the 20th century. For various applications – boilers, gas turbines, and aero-engines – it has remained a subject of intense study to the present day. An enormous amount of work has been performed on developing combustion diagnostics and studying combustion instabilities. This chapter outlines the most relevant work to the present study of flame dynamics.

2.1 Diagnostics

Several diagnostic methods were used in this study to quantify combustion properties. Absorption spectroscopy was used as a dynamic measurement of product gas temperature and equivalence ratio. Semiconductor lasers, probing two water transitions, were used to measure gas temperature. Equivalence ratio was measured through methane absorption of an infrared, helium-neon laser. Chemiluminescence was used as a measure of the chemical heat release of the combustion process.

2.1.1 Semiconductor Lasers. Enjoying widespread use in the telecommunications market, room-temperature semiconductor lasers have become robust, relatively inexpensive, and widely available. Lasers are currently available in wavelengths from 635 to 1650 nm [1]. The ability to rapidly tune the wavelength of diode lasers makes them attractive for spectroscopy applications. Recently, diode lasers have become available further in to the infrared, allowing access to stronger absorption bands. Allen gives a review of the many applications of semiconductor lasers in measuring species concentration, temperature, velocity, and mass flux [2].

The principle of operation of semiconductor lasers is discussed in several references [3-6]; and will only be summarized here. Radiation is produced in the active area region. In a Distributed Feedback (DFB) laser, the radiation oscillates between cleaved facets and over a small grating etched in to the bottom of the waveguide [7].

The laser is wavelength-tuned by altering the index of refraction of the active area. The index of refraction can be modified in two ways: case temperature and injection current. By controlling the temperature of the diode through a thermo-electric cooler (TEC), the laser frequency is shifted approximately 15 GHz/°C. Since the temperature of the entire diode, casing, and TEC must be controlled, tuning through the case temperature results in a slow tuning rate. Thus, it is often used when establishing and maintaining the wavelength of the diode laser.

Diode lasers can also be wavelength-tuned through the injection current, raising the temperature of the active area through Joule heating. By controlling the injection current into a diode laser, the emission frequency can be shifted approximately 0.5 GHz/mA. Since only the active area temperature is changed, the tuning rate is much faster. Current modulation is used for to dither the wavelength of diode lasers at rates of up to 10 kHz. Current modulation is often used to scan the laser over an absorption feature as discussed in Appendix B2.

2.1.2 Absorption Spectroscopy. Molecules tend to rotate and vibrate at select frequencies due to their geometry, just as a spring-mass-damper system has a natural frequency. Thus, the energy of the molecule is concentrated at these frequencies, and the molecule will absorb energy at these so-called transitions. Infrared spectroscopy is concerned with the vibratory motions of molecules caused by changes in configuration [8], as seen in Figure 2.1.

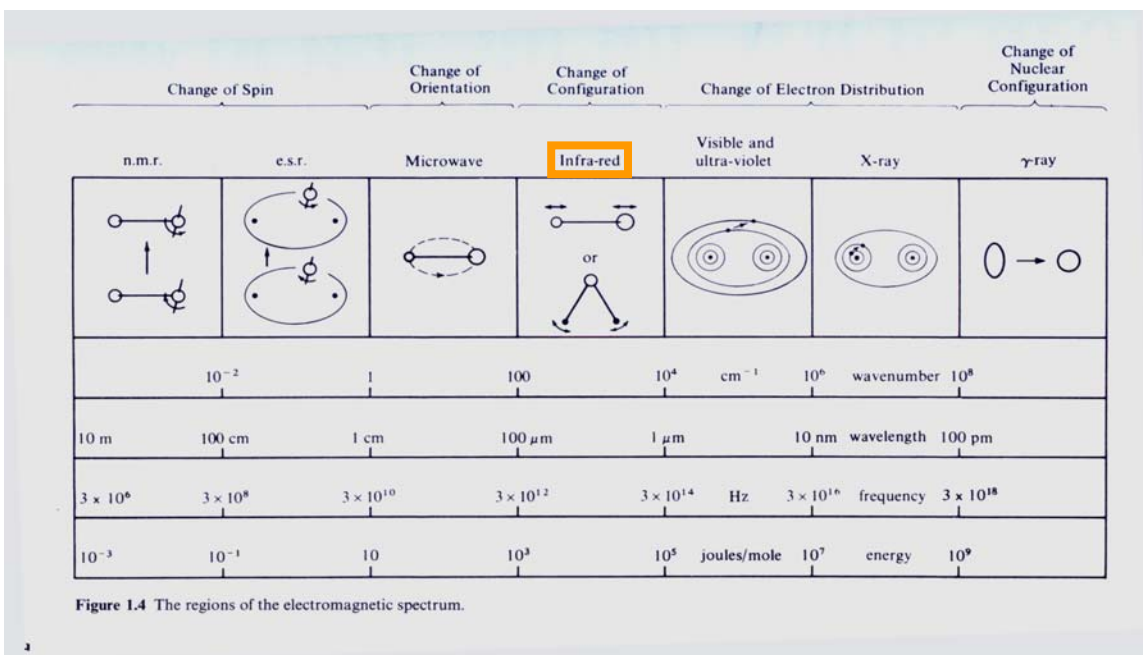


Figure 2.1. Modes of Vibration. The mode of vibration determines the wavelength of emission or absorption, image from [8].

The absorption of molecules is dependent on concentration, temperature, pressure, and the other constituents of the mixture, as discussed in Section 1.3.2. Since molecules absorb energy at select frequencies, the absorption of coherent light sources at these frequencies, or transitions, can be used to deduce the properties of specific species in a mixture. Absorption spectroscopy allows frequency-resolved measurements, as it is an optical technique with very small time constants. In the case of this study, absorption techniques are used to measure methane concentration and gas temperature.

Gas temperature was measured through probing two water transitions at 7185.59 cm^{-1} and 7444.37 cm^{-1} in this study (see Section 3.3.1). The line intensities and collisional broadening coefficients of the 7185.596 cm^{-1} (1391.67 nm) transition were experimentally verified by Lepere et al [9]. Furlong used Tunable Diode Laser Absorption Spectroscopy (TDLAS) to measure gas temperature and species concentration on a ducted Hencken burner [10]. Two DFB lasers were current-tuned across H_2O transitions at 7444.37 cm^{-1} ($\nu_1+\nu_3$ band) and 7185.59 cm^{-1} ($2\nu_1, \nu_1+\nu_3$ bands). Temperature was determined by the ratio of peak absorbances. The temperature

with the peak absorbance of one transition was used to measure H₂O concentration. The mean temperature and amplitude of temperature oscillations were controlled by through the primary fuel supply. In 1998, Furlong demonstrated control on a 5-kW, atmospheric pressure, non-premixed, annular dump combustor.

Temperature was measured, via H₂O absorption, on a model scramjet combustor [11]. In a similar manner, temperature was measured using two transitions near 1992 nm [12]. The TDLAS measurements were found to agree to within 2.9% of thermocouple measurements.

Absorption spectroscopy has also been used to measure the variations of equivalence ratio with time. Methane exhibits many strong transitions in the infrared region. Most notably, the transition at 3392 nm corresponds to the emission of an infrared Helium-Neon laser. The absorption method has been used to measure methane concentrations in the atmosphere [13], internal combustion engines [14], and experimental combustors [15]. As will be discussed in section 2.2.2, equivalence ratio variations play an important role in combustion instabilities.

2.1.3 Chemiluminescence. The light emitted from excited radicals in the flame, or chemiluminescence, has been widely used to infer flame properties. It is an optical method, and can therefore withstand the harsh conditions inside a combustor. It is also an emissions measurement, so no coherent light source is needed. Simple molecules are preferred, as their emission spectra are uncomplicated, sometimes a single peak. More complicated molecules have more complex spectra, and are more difficult to measure. Figure 2.2 shows a typical chemiluminescence spectrum for a Bunsen-type flame.

The use of chemiluminescence has been widespread. Clark [16] correlated OH*, CH*, CO₂*, and C₂* chemiluminescence to flow rate, fuel type, and equivalence ratio as early as 1958. The first dynamic measurements were performed by Price and Hurlle [17, 18], to relate noise from turbulent flames to C₂* and CH* emissions. More recently, the dynamic behavior of flames was studied using spatially-resolved, phase-locked measurements of OH* chemiluminescence as an indicator of chemical reaction rate [19].

In recent times, much work has been done to relate chemiluminescence to heat release rate. C₂* was used as an indicator of heat release rate [20]. Langhorne

presented a calibration of C_2^* to heat release rate [21]. CO_2^* chemiluminescence has also been used as an indicator of heat release rate [22]. Najm measured OH^* chemiluminescence, OH laser-induced fluorescence, and HCO laser-induced fluorescence and found HCO to be a good indicator of heat release rate in all types of flames [23]. Haber focused on the relationship between OH^* chemiluminescence and heat release rate. OH^* chemiluminescence was shown to be an accurate indicator of chemical heat release rate in the steady-state [24] as well as dynamically [25].

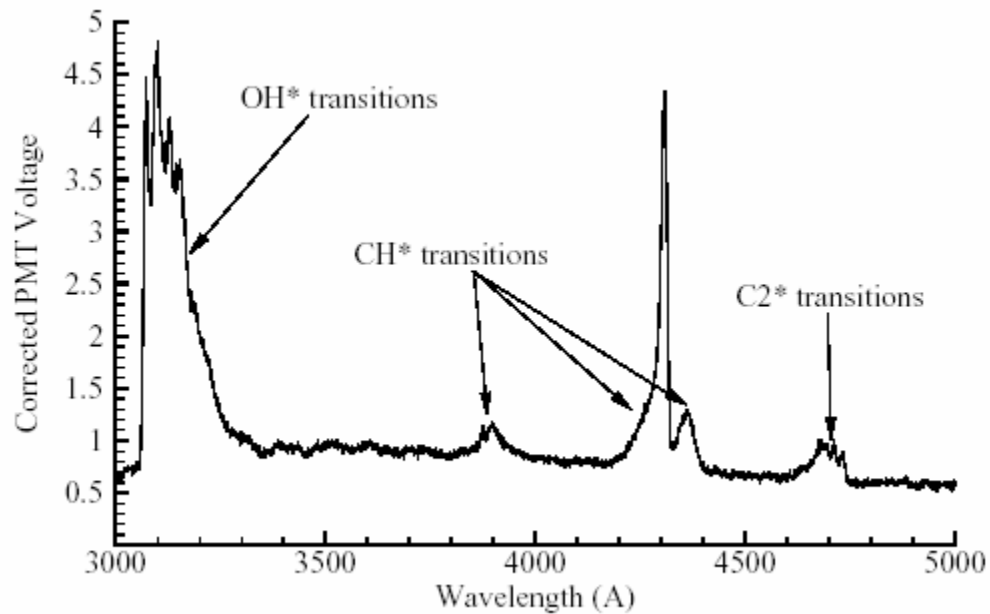


Figure 2.2. Chemiluminescence Spectrum. The spectrum was measured on a Bunsen-type flame [26].

2.2 Combustion Instabilities

Combustion instability research has a long history. Lord Rayleigh first explained combustion instabilities scientifically in 1878 [27], with his criterion that has become famous in the combustion community:

“If heat be periodically communicated to, and abstracted from, a mass of air vibrating (for example) in a cylinder bounded by a piston, the effect

produced will depend upon the phase of the vibration at which the transfer of heat takes place. If the heat is given to the air at the moment of greatest condensation, or be taken from it at the moment of greatest rarefaction, the vibration is encouraged. On the other hand, if heat be given at the moment of greatest rarefaction, or abstracted at the moment of greatest condensation, the vibration is discouraged.”

The criterion is still widely used, and expressed mathematically as the Rayleigh index

$$R = \int_0^T p'(t)q'(t)dt \quad (2.1)$$

where $p'(t)$ is the fluctuation in pressure, $q'(t)$ is the fluctuation in heat release rate, and T is the period of the oscillation. A positive Rayleigh index indicates amplification of the oscillation while a negative index indicates attenuation.

The simplest demonstration of combustion instabilities, and thus one of the most-studied systems, is the Rijke tube. In a Rijke tube, a heat source, usually a flame, is placed in a tube open at both ends. As seen in Figure 2.3, if the flame is placed in the lower quarter of the tube, the pressure and velocity are in phase making the Rayleigh index positive, and the oscillation grows to a self-excited limit cycle. It is assumed that the heat release rate varies approximately with the velocity. Raun provides an excellent review of Rijke tube work to date [28].

Under increasing pressure to lower emissions, lean-premixed combustion gained popularity in gas turbines. Lean combustion decreases flame temperatures, and therefore significantly lowers NO_x and CO levels. However, the flame operates near the limits of flammability, and is prone to instabilities. Many mechanisms of the cause of combustion instabilities have been proposed, including parametric flame instabilities, hydrodynamic instabilities, pulsating instabilities, and periodic extinction [29]. The main influences on combustion instabilities are variations in mass flow, variations in equivalence ratio, large-scale fluid structures, and random noise.

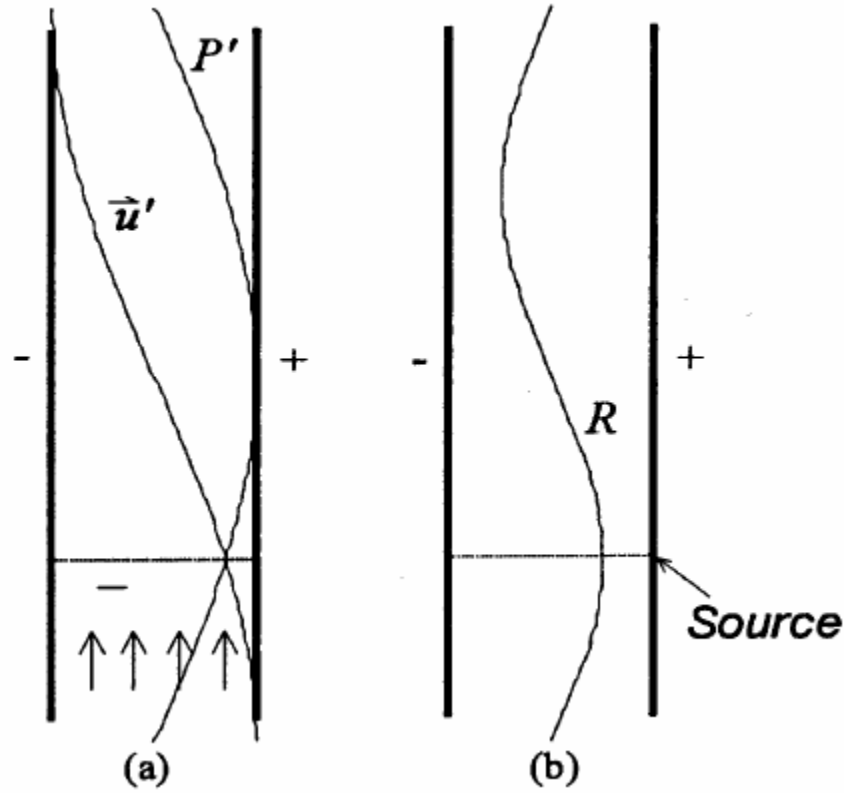


Figure 2.3. Rijke Tube Stability. When (a) the velocity and pressure fluctuations are in phase, (b) a positive Rayleigh index indicates growth of the oscillation [from [30]].

Analytical Work. In the past, simple models of flame dynamics have been used to predict thermoacoustic instabilities. Assuming constant flame speed, S_u , Annaswamy [31] used a first-order model of flame dynamics

$$\dot{q}'_0 + b_1 q'_0 = b_2 u'_0 \quad (2.2)$$

where q'_0 is the unsteady component of instantaneous heat release rate, u'_0 is the unsteady velocity. The constants b_1 and b_2 are based on the geometry and flame speed of the mixture. Rook [33] used a flamelet model to simulate the movement of the flame, arriving at a flame dynamics model that exhibits resonance

$$\frac{u'_b}{u'_u} = 1 + \left(\frac{\bar{T}_b - T_u}{T_u} \right) A(\hat{\omega}) + \frac{T_{ad} - \bar{T}_b}{T_u} \frac{1 - A(\hat{\omega})}{i\hat{\omega}} \frac{1}{2} (1 + \sqrt{1 + 4i\hat{\omega}}). \quad (2.3)$$

Dowling assumed heat release rate is proportional to the unsteady area variation of the flame [34] and arrived at a simple time-delay model

$$q'(t) = \frac{\bar{q}}{u_{z,inlet}}(t - \tau). \quad (2.4)$$

Schuller also assumed heat release rate to be proportional to the flame area fluctuations, resulting in a second-order model for conical flames,

$$F_{UCO}(\omega_*) = \frac{2}{\omega_*^2} [1 - \exp(i\omega_*) + i\omega_*] \quad (2.5)$$

where $\omega_* = (\omega R)/(S_L \cos \alpha)$ [35]. All of the previous models assume that the heat release rate is entirely dependent on the flame area, and thus only a function of chemical heat release rate. McIntosh includes convection and thermal diffusion in the model of flame dynamics. Assuming unity Lewis numbers, McIntosh [32] modeled flame dynamics as

$$\frac{u'_b}{u'_u} = 1 + \frac{(1 - T_{01}) \left(\frac{1}{2} + r \right) \exp \left[- \left(\frac{1}{2} + r \right) x_{l,fl} \right]}{2T_{01} \left[r \exp(-2rx_{l,fl}) + \omega / \Theta_1 (1 - T_{01}) \right]} \quad (2.6)$$

where T_{01} is the ratio of upstream gas temperature to initial flame temperature, $x_{f,fl}$ is the dimensionless stand-off distance, and Θ_1 is the dimensionless activation energy.

Experimental Work. Several researchers have worked to experimentally measure flame dynamics. Experimental flame dynamics work has also focused on chemical heat release through using chemiluminescence as an indicator of heat release rate. Khanna [36] measured the response of a laminar, flat-flame burner and a turbulent, swirl-stabilized combustor to velocity fluctuations using OH* chemiluminescence as an indicator of heat release rate. Both combustors were nominally stable and forced via a loudspeaker. The laminar flame exhibited two dominant resonances. One resonance was theorized to be dependent on mean energy content. The higher frequency resonance was attributed to chemical reaction rate. Kruger [37] measured the response of a full-scale industrial combustor via changes in acoustic impedance. The measured flame transfer functions were fit to a simple time-delay model. Lieuwen [38] studied flame dynamics on a self-excited combustor, using CH* chemiluminescence as an indicator of heat release rate. A nonlinear, saturation response in chemiluminescence was observed at

high frequencies of acoustic driving. Lawn [39] observed two resonances in swirl-stabilized flames, using OH* chemiluminescence. By acoustically forcing a flame at frequencies away from the natural instability, the empirical flame model was developed for turbulent flames

$$\frac{\hat{q}(x)}{\bar{q}(x)} = \frac{1}{iSt} \left(1 + \frac{e^{-i\beta St}}{iSt} \right) \frac{\hat{u}_G}{\bar{u}_G} e^{-i\omega\tau(x)} \quad (2.7)$$

where St is the Strouhal number, q is the heat release rate, u_G is the velocity, and “ $\hat{}$ ” denotes the amplitude of the fluctuating component while “ $\bar{}$ ” denotes the mean value [40].

2.2.1 Acoustics. Recent numerical and analytical work by Lieuwen shows that the temperature gradient in a flame has the effect of producing evanescent, spherical waves. A numerical study of a conical flame is compared with a 1-D analytical model [41]. The generation of vorticity by a planar wave interacting with a premixed flame was first demonstrated by Batley [42]. Sujith studied the effect of a temperature gradient on 1-D acoustic fields [43]. Lieuwen also investigated the effect of turbulent flames on an acoustic field [44].

2.2.2 Equivalence Ratio Fluctuations. The acoustics is thought to couple in to the unsteady heat release rate through two routes. A fluctuating mass flow rate will cause an unsteady heat release rate. A varying mixture strength, or equivalence ratio, will also cause an unsteady heat release rate. In gas turbines, the fuel nozzles are often choked to prevent the acoustics of the inlet tubing from interacting with the combustor. In the presence of an oscillating flow of oxidizer caused by pressure perturbations, a constant fuel flow would result in a varying equivalence ratio. Through methane absorption of an infrared Helium-Neon laser (3.39 μm), equivalence ratio fluctuations were measured during unstable combustion. The equivalence ratio variations were then correlated to chemiluminescence-based (CO₂*) heat release rate measurements [15]. The measurement technique is discussed in detail by Yoshiyama [14]. Methane concentration has also been measured using a Nd:YAG laser at 1.34 μm [45] and with a distributed feedback InGaAsP laser diode at 1.31 μm [46].

2.2.3 Fluid Mechanics and Turbulence. Turbulent combustion differs from laminar combustion in that diffusion and buoyancy-driven processes no longer govern. The flame speed and thermal diffusivity are affected by stretching and turbulence. The flame is anchored, usually, through use of large-scale fluid structures. Recirculation preheats the incoming reactants in the place of heat transfer from the ceramic or tube. Turbulence dramatically increases mixing. Many current combustors, as well as the turbulent combustor characterized in this study, use a large swirl, or tangential, velocity component to stabilize the flame. A swirl number, the non-dimensional ratio of axial flux of tangential momentum to axial momentum, characterizes swirling flows. With simplifications to eliminate the need for a static pressure measurement, the swirl number is defined as

$$S = \frac{\int_{R_e}^{R_o} \rho u_z u_\theta 2\pi r^2 dr}{\int_{R_e}^{R_o} \rho \left(u_z^2 - \frac{u_\theta^2}{2} \right) 2\pi R_o r dr} \quad (2.8)$$

where u_z is the axial velocity and u_θ is the tangential velocity [47]. Several experimental studies have been conducted on swirl-stabilized flames. Kulsheimer and Buchner compared flame transfer functions of jet flames and swirl-stabilized flames, observing instances when the fluctuations of the fluid structures became coherent with the excitation [48]. Paschereit took phase-locked images of OH* emissions corresponding to axisymmetric and helical modes of instability in a swirl-stabilized flame [49]. Lawn performed a similar study, observing the effect of axial distribution of heat release fluctuations and convection velocity on the instability [39].

Bibliography

1. Wolfrum, J., *Lasers in combustion: from basic theory to practical devices*. Proceedings of the 27th International Symposium on Combustion, 1998: p. 1-41.
2. Allen, M.G., *Diode laser absorption sensors for gas-dynamic and combustion flows*. Measurement Science Technology, 1998. **9**: p. 545-562.
3. Yariv, A., *Quantum Electronics*. 1975, New York: John Wiley & Sons.

4. Baer, D.S., et al., *Scanned- and fixed-wavelength absorption diagnostics for combustion measurements using multiplexed diode lasers*. AIAA Journal, 1996. **34**: p. 489-493.
5. Baer, D.S., et al., *Advanced diode-laser absorption sensors for combustion monitoring and control*. Proceedings of Spie - the International Society for Optical Engineering, 1999. **3535**: p. 16-23.
6. Wang, J., *New strategies of diode laser absorption sensors*, in *Mechanical Engineering*. 2001, Stanford University: Stanford, CA.
7. Furlong, E.R., *Diode-laser absorption spectroscopy applied for the active control of combustion*, in *Mechanical Engineering*. 1998, Stanford University: Stanford, CA.
8. Banwell, C.N. and E.M. McCash, *Fundamentals of Molecular Spectroscopy*. 1994, London: McGraw-Hill.
9. Lepere, M., et al., *Diode-laser spectroscopy: line profiles of H₂O in the region of 1.39 μ m*. Journal of Molecular Spectroscopy, 2001. **208**: p. 25-31.
10. Furlong, E.R., et al., *Combustion sensing and control using wavelength-multiplexed diode lasers*. AIAA, 1997. **97-0320**.
11. Upschulte, B.L., M.F. Miller, and M.G. Allen, *Diode laser sensor for gasdynamic measurements in a model scramjet combustor*. AIAA, 2000: p. 1246-1251.
12. Mihalcea, R.M., *CO and CO₂ measurements in combustion environments using external cavity diode lasers*, in *Mechanical Engineering*. 1999, Stanford University: Stanford, CA.
13. McManus, J.B., et al., *Field measurements of atmospheric methane with a HeNe laser-based real-time instrument*. Optical Methods in Atmospheric Chemistry, 1992. **1715**: p. 138-142.
14. Yoshiyama, S., et al., *Measurement of hydrocarbon fuel concentration by means of infrared absorption technique with a 3.39 μ m He-Ne laser*. JSAE Review, 1996. **17**: p. 339-345.
15. Lee, J.G., K. Kim, and D. Santavicca, *Measurement of equivalence ratio fluctuation and its effect on heat release during unstable combustion*. Proceedings of the Combustion Institute, 2000. **28**.
16. Clark, T., *Studies of OH, CO, CH and C₂ radiation from laminar and turbulent propane-air and ethylene-air flames*, in *NACA Technical Note*. 1958.
17. Price, R., I. Hurle, and T. Sugden, *Optical studies of the generation of noise in turbulent flames*. Proceedings of the Combustion Institute, 1968. **12**: p. 1093-1102.
18. Hurle, I., et al., *Sound emission from open turbulent premixed flames*. Proceedings of the Royal Society, 1968. **303**(Series A): p. 409-427.
19. Paschereit, C.O. and W. Polifke, *Investigation of the thermoacoustic characteristics of a lean premixed gas turbine burner*. Proceedings of the IGTI, 1998. **98-GT-582**.
20. Cho, S., K. Kim, and S. Lee, *Characteristics of thermoacoustic oscillation in a ducted flame burner*. Proceedings of the 36th Aerospace Sciences Meeting and Exhibit AIAA, 1998. **98-0473**.
21. Langhorne, P., *Reheat buzz: An acoustically coupled combustion instability. Part 1. Experiment*. Journal of Fluid Mechanics, 1988. **193**: p. 417-443.

22. Samaniego, J., F. Egolfopoulos, and C. Bowman, *CO₂* chemiluminescence in premixed flames*. Combustion Science and Technology, 1995. **109**: p. 183-203.
23. Najm, H., et al., *On the adequacy of certain experimental observables as measurements of flame burning rate*. Combustion and Flame, 1998. **113**: p. 312-332.
24. Haber, L., et al., *An examination of the relationship between chemiluminescence and heat release rate under non-adiabatic conditions*. IGTI Turbo Expo, 2000(2000-GT-0121).
25. Haber, L. and U. Vandsburger. *Combustion and heat transfer dynamics in a premixed laminar flat-flame burner*. in *Aerospace Sciences Meeting*. 2004.
26. Haber, L., et al., *An Examination of the Relationship between Chemiluminescence and Heat Release Rate Under Non-Adiabatic Conditions*. 2000.
27. Rayleigh, L., *The explanation of certain acoustical phenomena*. Royal Institution Proceedings, 1878. **8**: p. 536-542.
28. Raun, R.L., et al., *A review of rijke burners, and related devices*. Progress in Energy and Combustion Science, 1993. **19**: p. 313-364.
29. Candel, S. and T. Poinsot, *A tutorial on acoustics*. 1987, CNRS, Ecole Centrale des Arts et Manufactures: Chatenay-Malabry, France.
30. Khanna, V., *A study of the dynamics of laminar and turbulent fully and partially premixed flames*, in *Mechanical Engineering*. 2001, Virginia Tech: Blacksburg, VA.
31. Annaswamy, A.M., et al., *A feedback model of thermoacoustic instability in combustion processes*. 1997.
32. McIntosh, A.C., *Pressure disturbances of different length scales interact with conventional flames*. Combustion Science and Technology, 1991. **75**: p. 287-309.
33. Rook, R., et al., *Response of burner-stabilized flat flames to acoustic perturbations*. Combustion Theory and Modeling, 2002. **6**: p. 223-242.
34. Dowling, A.P. and S. Hubbard, *Instability in lean premixed combustors*. IMechE, 2000. **214**: p. 317-332.
35. Schuller, T., D. Durox, and S. Candel, *A unified model for the prediction of laminar flame transfer functions: comparisons between conical and V-flame dynamics*. Combustion & Flame, 2003. **134**: p. 21-34.
36. Khanna, V.K., et al., *Dynamic analysis of burner stabilized flames part I: laminar premixed flames*. American Flame Research Committee (AFRC) International Symposium, 2000.
37. Kruger, U., et al., *Prediction and measurement of thermoacoustic improvements in gas turbines with annular combustion systems*. Journal of Engineering for Gas Turbines and Power, 2001. **123**: p. 557-566.
38. Lieuwen, T. and Y. Neumeier, *Nonlinear pressure-heat release transfer function measurements in a premixed combustor*. Proceedings of the Combustion Institute, 2002. **29**.
39. Lawn, C.J., *The thermo-acoustic response of a premixed swirl burner*. Proceedings of the Institute of Mechanical Engineers, 2000. **214**: p. 333-354.
40. Bloxsidge, G.J., A.P. Dowling, and P. Langhorne, *Reheat buzz - an acoustically coupled combustion instability, part II theory*. Journal of Fluid Mechanics.

41. Lee, D. and T. Lieuwen, *Premixed flame kinematics in a longitudinal acoustic field*. AIAA/ASME/SAE/ASEE Joint Propulsion Conference, 2001. **AIAA-01-3851**.
42. Batley, G.A., et al., *A numerical study of the vorticity field generated by the baroclinic effect due to the propagation of a planar pressure wave through a cylindrical premixed laminar flame*. Journal of Fluid Mechanics, 1994. **279**: p. 217-237.
43. Sujith, R.I., G.A. Waldherr, and B.T. Zinn, *An exact solution for one-dimensional acoustic fields in ducts with an axial temperature gradient*. Journal of Sound and Vibration, 1995. **184**(3): p. 389-402.
44. Lieuwen, T., *Theory of high frequency acoustic wave scattering by turbulent flames*. Combustion and Flame, 2001. **126**: p. 1489-1505.
45. Scott, J.C., R.A.M. Maddever, and A.T. Paton, *Spectroscopy of methane using a Nd:YAG laser at 1.34 μm* . Applied Optics, 1992. **31**(6): p. 815-821.
46. Silveira, J.P. and F. Grasdepot, *New signal processing for wavelength modulation spectroscopy: application to an industrial methane sensor*. Infrared Physics and Technology, 1996. **37**: p. 143-147.
47. Ribeiro, M.M. and J.H. Whitelaw, *Coaxial jets with and without swirl*. Journal of Fluid Mechanics, 1980. **96**(4): p. 769-795.
48. Kulsheimer, C. and H. Buchner, *Combustion dynamics of turbulent swirling flames*. Combustion and Flame, 2002. **131**: p. 70-84.
49. Paschereit, C.O., E. Gutmark, and W. Weisenstein, *Excitation of thermoacoustic instabilities by interaction of acoustics and unstable swirling flow*. AIAA, 2000. **38**(6): p. 1025-1034.